PHYSICS OF THE JOVIAN MAGNETOSPHERE

Edited by A. J. DESSLER
Department of Space Physics and Astronomy
Rice University

CAMBRIDGE UNIVERSITY PRESS

Cambridge
London New York New Rochelle
Melbourne Sydney

Published by the Press Syndicate of the University of Cambridge
The Pitt Building, Trumpington Street, Cambridge CB2 1RP
32 East 57th Street, New York, NY 10022, USA
296 Beaconsfield Parade, Middle Park, Melbourne 3206, Australia

First published 1983

Printed in the United States of America

Library of Congress Cataloging in Publication Data

Main entry under title:

Physics of the Jovian magnetosphere.

(Cambridge planetary science series)

Includes index.

1. Jupiter (Planet)–Atmosphere.
2. Magnetosphere. I. *Dessler, A. J.*

QB661.P47 538'.766'099925 81-21752
ISBN 0 521 24558 3 AACR2

CONTENTS

TABLES

1

JUPITER'S MAGNETIC FIELD AND MAGNETOSPHERE

Mario H. Acuña, Kenneth W. Behannon, and J. E. P. Connerney

Jupiter has a magnetic moment second only to that of the Sun's. Estimates of dipole magnitude range from 4.208–4.28 G-R_J^3. The dipole is found to be tilted $\sim 9.6°$ to the rotation axis toward $\sim 202°$ System III (1965) longitude in the northern hemisphere. Jupiter also possesses substantial quadrupole and octupole moments, which implies that the interior sources of the field lie nearer the surface than in the case of Earth. The internally-produced field dominates the inner magnetosphere out to a distance of $\sim 6\ R_J$, the orbital distance of Io, where measurement of perturbation magnetic fields yields an estimated 2.8×10^6 A for the current flowing in the Alfvén current tube linking Io with the Jovian ionosphere. The middle magnetosphere of Jupiter, extending from $\sim 6\ R_J$ to 30–50 R_J, is dominated by an equatorial azimuthal current disc. When the disc is modeled as a 5 R_J thick annular current sheet extending from 5 to 50 R_J, a fit to spacecraft data requires a current density of $\sim 5 \times 10^6$ A/R_J^2 at the inner edge of the annulus. An asymmetric longitudinal variation in the radial component of the magnetic field in this region provides evidence for a thickening of the magnetodisc on the dayside. Between the outer edge of the disc and the sunward magnetopause, which can vary in distance from $\sim 45\ R_J$ to $\sim 100\ R_J$ there is a "buffer" zone which is very sensitive to variations to external pressure. The field there is southward on average, but highly variable in both magnitude and direction on timescales less than one hour, especially near the magnetopause. On the nightside of the planet, a magnetic tail of radius ~ 150–$200\ R_J$ and length of probably a few AU is formed in the interaction of the solar wind with the Jovian magnetosphere. The $\sim 5\ R_J$ thick current sheet separating the tail lobes is a night side extension of the magnetodisc, is on average parallel to the ecliptic plane and oscillates about the longitudinal axis of the tail as Jupiter rotates. In the dawn and tailward magnetosheath, the magnetic field has a predominant north–south orientation and varies between the two extremes with a quasiperiod of ~ 10 hr. There is strong correlation with the north–south plasma velocity components in those regions, suggesting convected wave production by the wobble of the flattened Jovian magnetosphere and current sheet system.

1.1. Introduction

Among the planets in the solar system, Jupiter is unique not only because of its immense size and mass and the variety of phenomena taking place in its environment, but also because of its large magnetic moment, second only to the Sun's. The Jovian magnetic field was first detected indirectly by radio astronomers who postulated its existence to explain observations of nonthermal radio emissions from Jupiter at decimetric and decametric wavelengths [see Chapter reviews and Carr and Gulkis, 1969; Carr and Desch, 1976; Berge and Gulkis, 1976; also de Pater, 1980b]. Some of the basic characteristics of the field were derived from these observations, such as its southward polarity, opposite Earth's, and the approximate value of the tilt angle between the magnetic dipole axis and the axis of rotation of the planet, determined to be $\sim 10°$. Coarse estimates were established for the surface field intensity and dipole moment based on trapped radiation models and the observed cutoff of decametric emissions at 40 MHz [Komesaroff, Morris, and Roberts, 1970; Carr, 1972a].

Since these early radio astronomical studies of the Jovian magnetosphere, four spacecraft, Pioneer 10 (1973), Pioneer 11 (1974), Voyager 1, and Voyager 2 (both

1979), have flown by the planet at close distances and have provided in situ information about the field geometry and its strength. The direct measurements confirmed the zeroth order models derived from the radio data and added a vast amount of new and detailed information about the global characteristics of the field, its dynamics and interaction with the solar wind. For detailed reviews of early results derived from ground based and the Pioneer 10 and 11 spacecraft observations the reader is directed to the book *Jupiter*, edited by Gehrels [1976], and to Smith and Gulkis [1979], Davis and Smith [1976], Acuña and Ness [1976a,b,c], and Carr and Gulkis [1969] and references therein.

As in the case of Earth, the magnetic field stands off the solar wind at a considerable distance from the planet, creating a giant magnetospheric cavity. If it were visible, the Jovian magnetosphere would appear from Earth to be the largest object in the sky. Viewed head on, its width would be about four times as large as the Moon or Sun. The boundary of this cavity comprises a detached bow shock wave, generated by the super-Alfvénic flow of the solar wind past the magnetized obstacle, a magnetosheath layer in which the deflected solar wind creates a turbulent flow regime, and a magnetopause "surface" at which internal magnetospheric pressure balances that associated with the impinging solar wind.

It has become customary to describe the Jovian magnetosphere in terms of three principal regions. The *inner magnetosphere* is the region where the magnetic field created by sources internal to the planet dominates, and contributions from current systems external to the planet are not significant. This region was initially defined as extending from the planetary surface to a distance of 10–15 R_J (Jovian radii), but recent results from the Voyager flybys indicate that the outer radius should be reduced to approximately 6 R_J, the orbit of Io. Outside of this region the effects of an azimuthal current sheet in the equatorial plane produce a significant perturbation, leading to the stretching of the magnetic field lines in the radial direction. The region in which the equatorial currents flow will be denoted as the *middle magnetosphere*, and in our definition, would extend from ~ 6 R_J to approximately 30–50 R_J where the asymmetry due to the magnetopause and tail current systems becomes important. In the *outer magnetosphere*, the field has a large southward component and exhibits large temporal and/or spatial variations in magnitude and direction in response to changes in solar wind pressure. This region extends from the magnetopause boundary to approximately 30–50 R_J, and includes as well the extensive Jovian magnetic tail.

In this chapter we shall present a description of the magnetic field in these three regions from the phenomenological point of view derived from spacecraft observations (predominantly the recent Voyager results) and the quantitative models which have been developed to date on the basis of these observations.

1.2. The inner magnetosphere

General description and mathematical models

As previously defined, the inner magnetosphere is that region where the magnetic field generated by currents flowing in the interior of the planet dominates. The timescale for field variations, both in magnitude and direction, is long, and the field is smoothly varying when observed from a spacecraft in a flyby trajectory. It is generally accepted that the magnetic-field-generation mechanism is a thermal-convection-driven dynamo operating in the electrically conducting regions of Jupiter's interior [Hide and Stannard, 1976; Gubbins, 1974; Busse, 1979]. Thus knowledge about the magnetic field provides means for studying Jupiter's interior [Smoluchowsky, 1975; Stevenson,

1974]. Beyond 6 R_J the effects of external currents become too significant to be neglected; hence, we have chosen this radius as the outer boundary.

Because the region of interest contains no significant sources (i.e., $\mathbf{J} = \nabla \times \mathbf{B} \simeq 0$), the magnetic field $\mathbf{B}$ can, to good approximation, be derived from a scalar potential function V which represents the contribution of sources internal and external to the region. Thus, we have

$$\mathbf{B} = -\nabla V = -\nabla(V^e + V^i) \tag{1.1}$$

The potential function V is the sum of an external potential V^e and an internal potential V^i and is generally expressed in terms of spherical harmonic functions, that is, solutions to Laplace's equation of the form [Chapman and Bartels, 1940]

$$V = V^e + V^i = a \sum_{n=1}^{\infty} \left(\frac{r}{a}\right)^n T_n^e + \left(\frac{a}{r}\right)^{n+1} T_n^i \tag{1.2}$$

This is the classical formulation for the potential originated by Gauss in 1830 and used in studies of the Earth's magnetic field [Gauss, 1877]. In our case, r denotes the distance from Jupiter's center and a is Jupiter's equatorial radius, (1 R_J = 71,372 km). (A general discussion of the representation of magnetic fields in space has been given by Stern [1976].)

The functions T_n^e and T_n^i are given with respect to the coordinate system defined below, as:

$$T_n^e = \sum_{m=0}^{n} P_n^m(\cos\theta)\,[G_n^m \cos m\phi + H_n^m \sin m\phi] \tag{1.3}$$

for the contribution due to exterior sources and

$$T_n^i = \sum_{m=0}^{n} P_n^m(\cos\theta)\,[g_n^m \cos m\phi + h_n^m \sin m\phi] \tag{1.4}$$

for the internal sources.

The angles ϕ and θ are the conventional right-handed polar coordinates and therefore denote Jovigraphic System III (1965.0) *east* longitude and colatitude respectively, $P_n^m(\theta)$ are associated Legendre functions with Schmidt normalization and g_n^m, h_n^m, G_n^m, H_n^m are the Schmidt coefficients. In some studies the external potential V^e has been expressed in an inertial (nonrotating) coordinate system [see Smith et al., 1975].

If we assume a magnetic field representation of the form (1.1), the development of a magnetic field model from a set of M observations along a spacecraft trajectory requires the determination of the coefficients g_n^m, h_n^m, G_n^m, and H_n^m up to order $n = n_{\max}$ ($n_{\max} < \infty$) that minimize the sum of the vector residuals squared

$$X^2 = \sum_{k=1}^{M} |\mathbf{B}_{\text{model}}{}^k - \mathbf{B}_{\text{obs}}{}^k|^2 = \sum_{k=1}^{M} |\epsilon_k|^2 \tag{1.5}$$

The order of the model, $n = n_{\max}$, represents the physical complexity associated with the mathematical formulation. From potential theory it is known that a unique

Table 1.1. *Spherical harmonic coefficients for models of the Jovian magnetic field (System III, 1965)*

Terms		O_4 (Acuña and Ness, 1976)	P 11(3,2)*A*, Davis et al. (1975)
Internal:	g_1^0	4.218	4.144
	g_1^1	−0.664	−0.692
	h_1^1	0.264	0.235
	g_2^0	−0.203	0.036
	g_2^1	−0.735	−0.581
	h_2^1	−0.469	−0.427
	g_2^2	0.513	0.442
	h_2^2	0.088	0.134
	g_3^0	−0.233	−0.047
	g_3^1	−0.076	−0.502
	h_3^1	−0.580	−0.342
	g_3^2	0.168	0.352
	h_3^2	0.487	0.296
	g_3^3	−0.231	−0.136
	h_3^3	−0.294	−0.041
External:	G_1^0		−194.6 (nT)
	G_1^1		68.7
	H_1^1		80.3
	G_2^0		5.6
	G_2^1		9.1
	H_2^1		− 9.4
	G_2^2		− 16.2
	H_2^2		− 8.3

representation of the magnetic field in a source-free region is derivable from vector measurements over a simple surface that completely encloses the internal sources. Because a spacecraft trajectory only constitutes a single curve in space, the solutions obtained are not unique, and cross coupling or mutual dependence among the Schmidt coefficients occurs.

From the above, it is clear that trajectories that maximize the range of latitudes and longitudes covered within the radial distances considered lead to more complete representations of the planetary field. The characteristics of a given trajectory can be used to determine the order of the model n_{max} that can be used to model the observations with acceptable physical credibility. A model of the planetary field incorporating

Table 1.2. *Characteristics of dipole terms for models of the Jovian magnetic field*[a]

Model	$\|M\|$	Tilt	λ_{III} (1965)
O_4	4.28	9.6°	201.7°
P 11(3,2)*A*	4.208	10°	198.8°

[a] For the characteristics of dipole terms derived from other models of the field the reader is referred to *Smith and Gulkis* [1979].

terms of order higher than n_{max} may fit the data exceedingly well along the spacecraft trajectory, but not elsewhere. Hence, the predictive properties and basic purpose of the model are rendered useless. Detailed discussions on the selection of n_{max} for given spacecraft trajectories and the physical validity of higher order models have been given by Acuña and Ness [1976b], Davis and Smith [1976], and Connerney [1981a]. The latter author in particular has applied generalized inverse techniques to the least-squares problem represented by Equation (1.5), which yield direct estimates of confidence levels associated with the Schmidt coefficients for a given spacecraft trajectory.

In the case of Jupiter, the best trajectory for planetary magnetic field studies was that provided by Pioneer 11. This was a high latitude retrograde flyby with a closest Jovicentric approach distance of 1.6 R_J. Although Pioneer 10 and Voyager 1 approached the planet to within 2.85 and 4.9 R_J respectively, their prograde trajectories remained close to the equatorial plane; Voyager 2 only came to within 10 R_J of Jupiter and thus did not contribute significant data for studies of the planetary field. However, these latter three spacecraft provided a wealth of information about the middle magnetosphere and hence, indirectly, about the radial distance range over which the spherical harmonic representation is valid [Davis and Smith, 1976; Ness et al., 1979a,b,c].

On the basis of the Pioneer 10 and 11 measurements [Smith et al., 1975; Acuña and Ness, 1976a,b,c], several models of the Jovian magnetic field were developed. Each of these reflects not only the many approaches that are possible in obtaining estimates for the spherical harmonic coefficients, but they also point to slight measurement differences in the respective observations [Acuña and Ness, 1976c; Davis and Smith, 1976; Connerney, 1981a]. Two principal models have emerged as "best" representing the planetary field in terms of spherical harmonics: the O_4 model of Acuña and Ness [1976a,c] and the P 11(3,2)*A* model of Davis, Jones, and Smith [1975] (see also Smith, Davis, and Jones [1976]). They have been tested against independent evidence from ground based radio observations and in situ energetic-charged-particle measurements. The latter provide information about the global characteristics of the field not obtainable from the local magnetic field measurements and hence lend physical credibility to the models [Acuña and Ness, 1976a,c; Smith and Gulkis, 1979]. Table 1.1 lists the Schmidt coefficients for both models. The O_4 model includes terms up to the octupole ($n_{max} = 3$) but no external terms ($G_n^m = H_n^m \equiv 0$). The P 11(3,2)*A* model also includes internal terms up to the octupole but adds external terms which include quadrupole coefficients ($n_{max}^{ext} = 2$). These coefficients have been transformed to the System III (1965) longitude system values. The characteristics of the dipole terms are given in Table 1.2.

The global characteristics of the field predicted by these models are illustrated in Figures 1.1 through 1.3 where the total field intensity, dip, and declination angles are shown in the form of isocontour maps at the surface of the planet and at 2 Jovian radii.

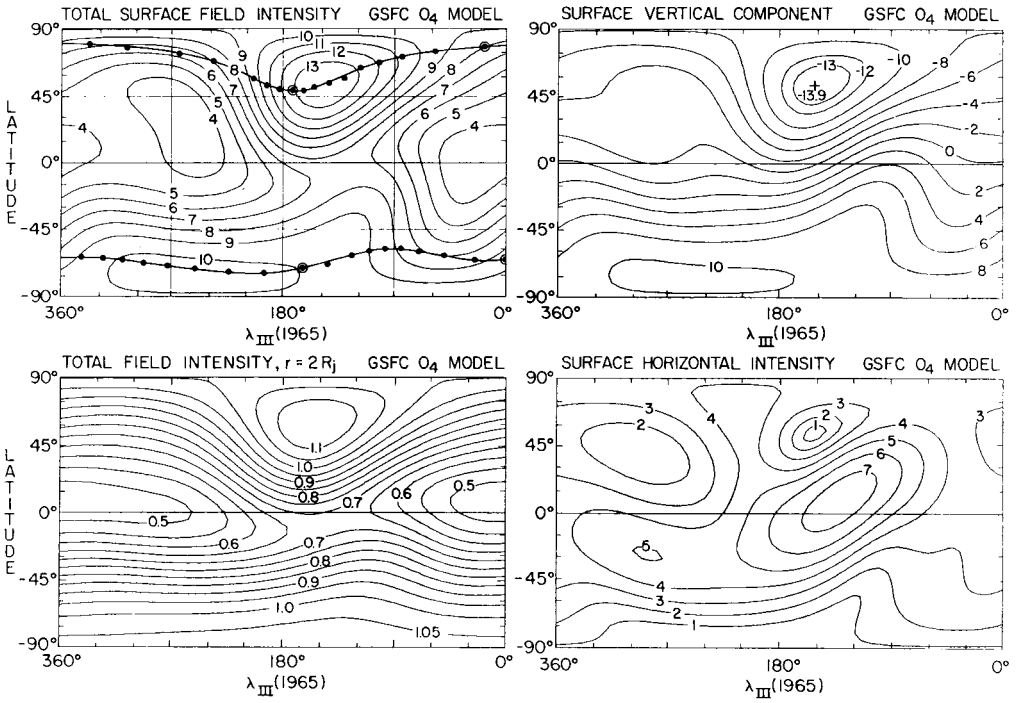

Fig. 1.1. Isocontour maps of total field intensity as predicted by the O_4 model at the surface and at 2 Jovian radii. The vertical and horizontal field intensities at the surface are also shown. Note that the dynamic flattening of 1/15.4 has been incorporated into the surface maps. Also shown in upper left panel are traces of the feet of the field line (flux tube) through Io (filled circles on solid curves).

The dip and declination angles are defined in the usual sense for Earth's case: dip = $\tan^{-1} Z/H$, where Z and H denote the local vertical (downward) and horizontal field components, respectively, and declination = $\tan^{-1} Y/X$, where X is the local field component directed towards the north and Y the local field component directed towards the east. Note that the surface maps take into account Jupiter's dynamic flattening, $f = 1/15.4$; those computed at 2 R_J assume a spherical surface. From the coefficients given in Table 1.1 and the maps shown in Figures 1.1 through 1.3 it is clear that Jupiter possesses substantial quadrupole and octupole moments which lead to a relatively complex field morphology extending to significant distances from the planet although the field is largely dipolar for distances as close as 2 R_J. On the surface the maximum field strength at the poles is asymmetrical, ~14 and 10.4 G in the north and south polar regions, respectively. The relatively large high-order terms also imply that the sources of the magnetic field, presumably in Jupiter's core, lie closer to the surface than in the case of the Earth.

A new estimate of Jupiter's planetary magnetic field has been obtained from the Voyager 1 observations. Connerney, Acuña and Ness [1982] combined an explicit model of the magnetodisc current system with a spherical harmonic model of the planetary field and obtained most of the parameters of an octupole internal field model. The resulting model fits the observations extremely well (Fig. 1.4) throughout the analysis interval ($r < 20\ R_J$) and is very similar to the octupole Pioneer 11 models. Comparing dipole parameters of the epoch 1979.2 Voyager 1 model with the epoch 1974.9 O_4 model, Connerney, Acuña, and Ness find no statistically significant change in Jupiter's dipole moment, tilt angle or longitude.

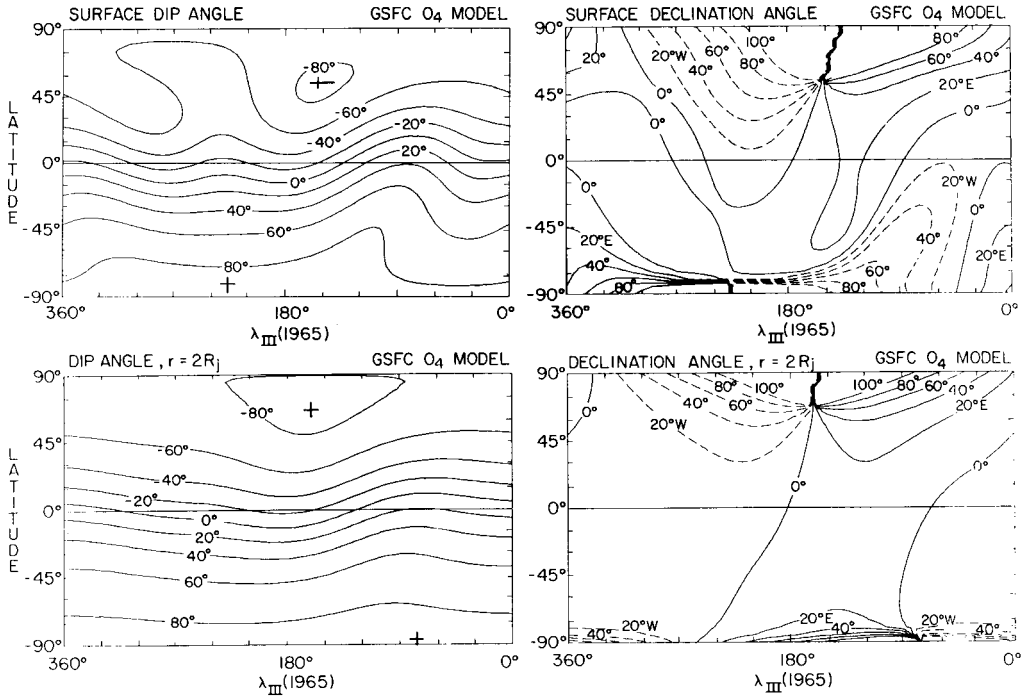

Fig. 1.2. Isocontour maps of declination and dip angles as predicted by the O_4 model for the surface and 2 Jovian radii. See text for the definition of these angles. A dynamic flattening of 1/15.4 has been incorporated into the surface maps.

Offset tilted dipole

A simplified model for the field can be obtained by fitting the data to a noncentered dipole. Alternatively, an offset, tilted dipole (OTD) representation can be derived from the quadrupole terms in the form given by Bartels [1936]. These offset, tilted dipole models of the Jovian field find application in problems that require a simple magnetic field model for computational ease and are not concerned with the detailed morphology of the field near the surface. A typical widely used offset, tilted dipole model is the D_4 model of Smith, Davis, and Jones [1976]; its characteristics are given in Table 1.3.

Table 1.3. *Characteristics of offset tilted dipole (OTD) models of the Jovian magnetic field*

Model	$\|M\|$	Tilt	λ_{III} (1965)	Offset (R_J)	δ^b	μ(1965)
D_4	4.225	10.8°	200.8°	0.101	5.1	155.6°
OTD[a]	4.35	9.5°	208.8°	0.068	−12.6°	174.2°
O_4	4.28	9.6°	201.7°	0.131	− 8.0°	148.57°
P 11(3,2)*A*	4.208	10°	198.8°	0.108	4.8°	143.07°

[a] Acuña and Ness [1976c].
[b] δ and μ are the latitude and longitude of the offset vector in System III (1965).

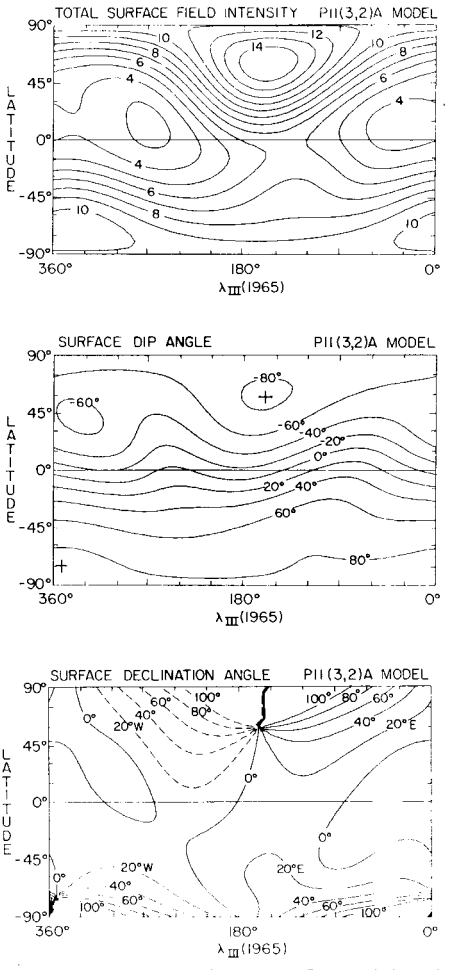

Fig. 1.3. Surface total field intensity, dip, and declination angles as predicted by the P 11(3.2)*A* model. See text for definition of the angles.

Also in the table are given the equivalent OTD models derived from the O_4 model and the P 11(3,2)*A*.

It can be argued that the OTD models represent the simplest morphological structure (dipole) associated with the planetary field. The degree of complexity is given by a measure of how far the real field deviates from this zeroth order representation. This has been illustrated in Figure 1.5 where we have plotted isointensity contours on the surface of the planet for the difference field between the O_4 and the OTD models of Acuña and Ness [1976c]. A strong quadrupolar component remains evident in this figure, indicative of a field complexity at the surface which cannot be adequately represented by OTD models.

An important point that must be kept in mind when using analytical models of planetary magnetic fields is their nonuniqueness. Magnetic field observations acquired along a flyby trajectory, for example, are insensitive to certain linear combination of parameters. This has been illustrated by the "invisible planet" constructed by Connerney [1981a] in connection with the Pioneer 11 flyby trajectory at Jupiter. This figure is reproduced in Figure 1.6 showing surface isocontour maps of Jovian model magnetic fields that would not have been detected by the magnetometers on Pioneer 11, assuming (Fig. 1.6*a*) a uniform noise distribution and (Fig. 1.6*b*) observation noise proportional to the local field magnitude.

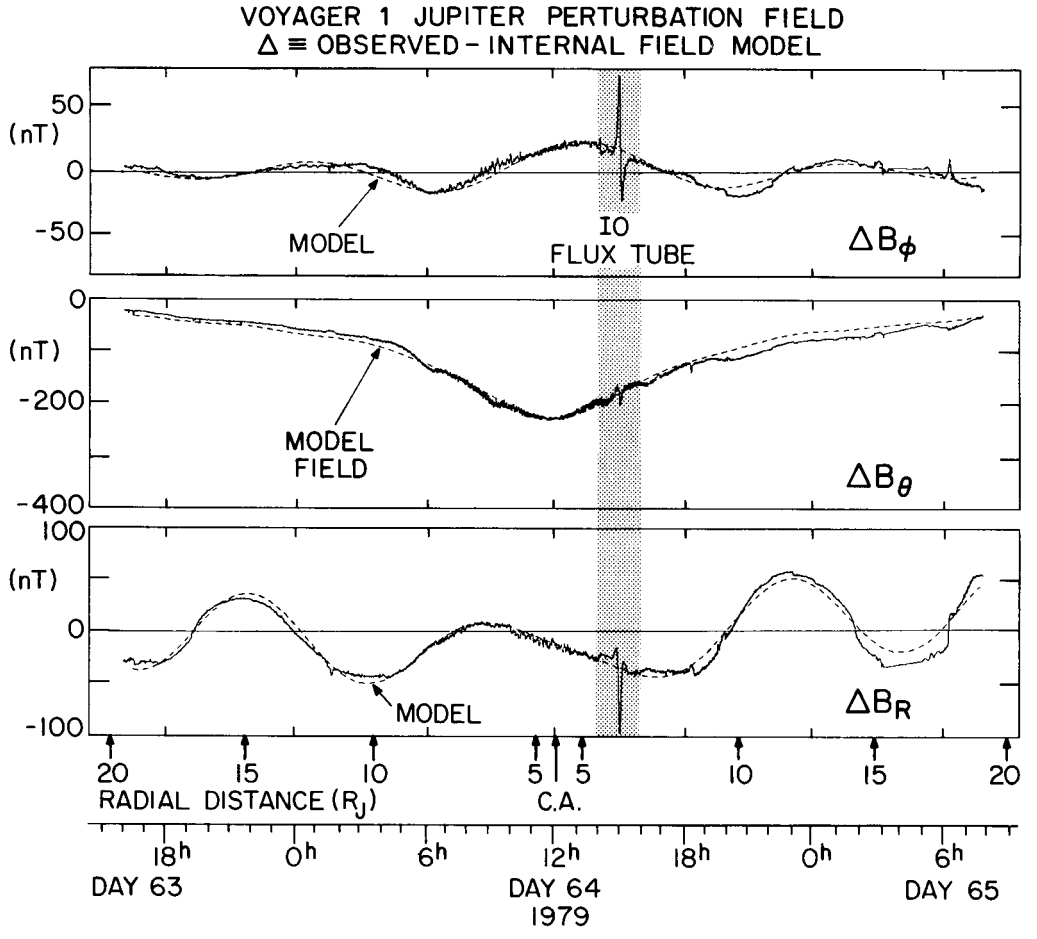

Fig. 1.4. Comparison of modeled magnetic field (dashed) with that observed for Voyager 1 (spherical coordinates are used). In this presentation the model internal field has been subtracted from the observations; the remaining model field (dashed) is due to Jupiter's magnetodisc currents. The total field at closest approach (C.A.) is ~3330 nT (from Connerney, Acuña, and Ness, 1982).

Magnetic field geometry relevant to energetic particle trapping

Energetic particles trapped in the Jovian magnetosphere serve as excellent tracers of the magnetic field morphology, since in their bounce and drift motions around the planet they trace out the magnetic field lines over a large region of space. Thus, energetic particle measurements aboard spacecraft play an important role in establishing the global characteristics of the field (see for example Van Allen et al. [1974a]), and in providing independent evidence against which the validity of the magnetic field models can be tested. The satellites in the Jovian system act to remove trapped energetic particles by absorption into their surfaces [Mead and Hess, 1973]. The observed absorption signatures and their relative locations with respect to the planet can be used effectively to infer characteristics of the magnetic field [Acuña and Ness, 1976c; Van Allen, 1976;

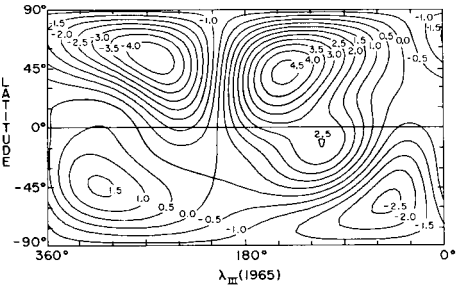

Fig. 1.5. Isocontour map of the differential in total surface field intensity computed by subtracting the OTD model of Acuña and Ness from the O_4 model. The large remaining quadrupolar and higher order contributions to the field cannot be adequately modeled by an offset, tilted dipole.

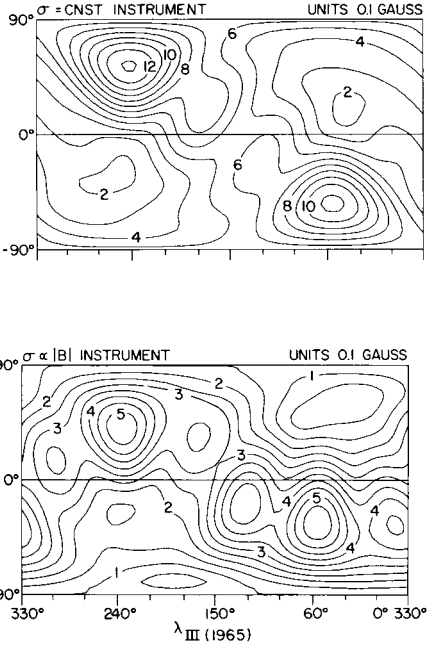

Fig. 1.6. "Invisible planet": Surface isointensity contour map of a Jovian model magnetic field that would not have been detected by a magnetometer on Pioneer 11: (a) (upper panel) assuming observations with a .005 G random noise component; (b) (lower panel) with a noise component proportional to the local field magnitude (see text). A dynamical flattening of 1/15.4 is assumed in the determination of the surface equipotential (from Connerney [1981a]).

Simpson and McKibben, 1976; Fillius, 1976]. Conversely, the magnetic field models in conjunction with observed energetic charged particle absorption effects can be used to infer the presence and properties of undetected absorbers such as unknown rings and satellites [Van Allen et al., 1980; Acuña and Ness, 1976c; Fillius, 1976].

It is important therefore to determine the adiabatic particle parameters for particle detectors aboard a given spacecraft and trajectory. For example, L-shells and equatorial pitch angles for charged particles incident from a given direction constitute extremely useful quantities. (For a detailed discussion of adiabatic particle motion and parameters in a planetary magnetic field the reader is directed to Roederer [1970]). An example of this type of calculation using the O_4 model is given in Figure 1.7 for the Pioneer 11 spacecraft encounter trajectory and for particles with pitch angles equal to 90° at the spacecraft. Also shown in the figure are the range of L-shells swept by Io and Amalthea, as predicted by several models, where absorption effects should be observed [Van Allen et al, 1974a; Fillius, Mogro-Campero, and McIlwain, 1975]. Note that the range of L-shells swept by these two satellites as they move around in their orbits is

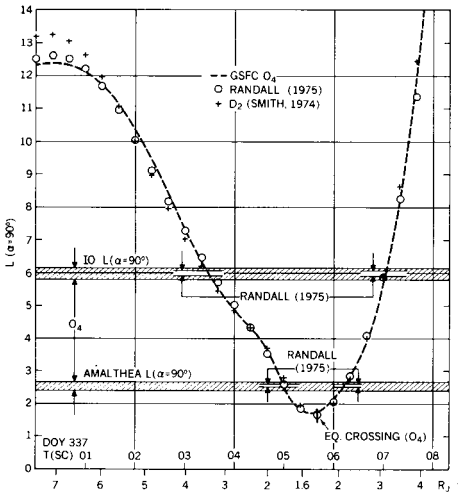

Fig. 1.7. McIlwain "*L*" parameter values computed for charged particles with 90° pitch angle at the spacecraft. The trajectory is that of Pioneer 11 at Jupiter. The shaded regions indicate the range of *L*-shells swept by the Jovian satellites Io and Amalthea, where particle absorption effects should be observable. See Van Allen [1976] for a description of the Randall (1975) model.

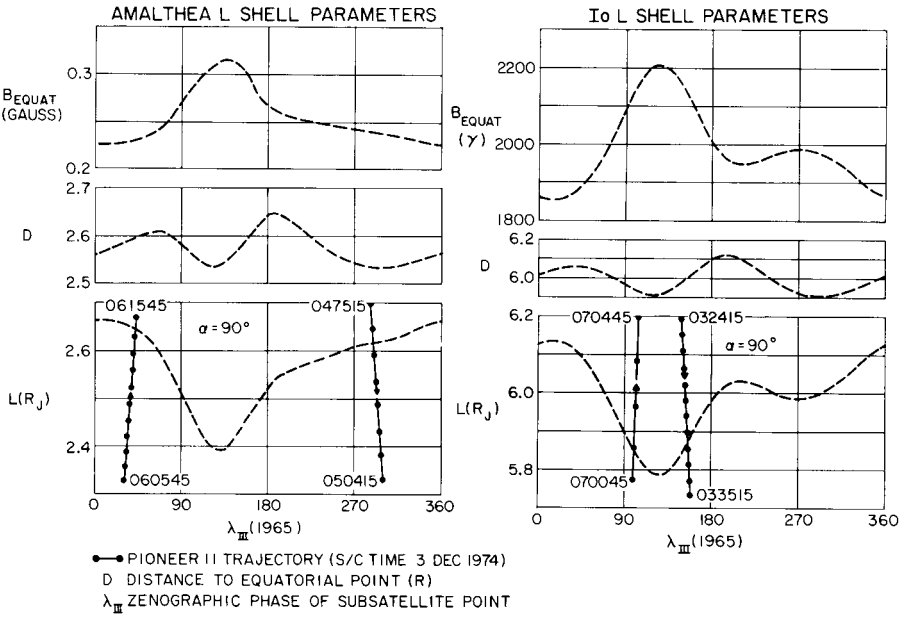

Fig. 1.8. *L*-parameter values computed for the "trajectories" (orbits) of Io and Amalthea around Jupiter. Note the large range of *L*-values which the satellites traverse around their orbits. The indicated longitude is System III (1965).

much broader for the O_4 and P 11(3,2)*A* models than predicted by dipole models [Acuña and Ness, 1976c], as illustrated in Figure 1.8. This effect becomes pronounced for satellites in the middle magnetosphere, such as Ganymede, where the field lines are stretched out radially by external currents. These effects are discussed in the next section.

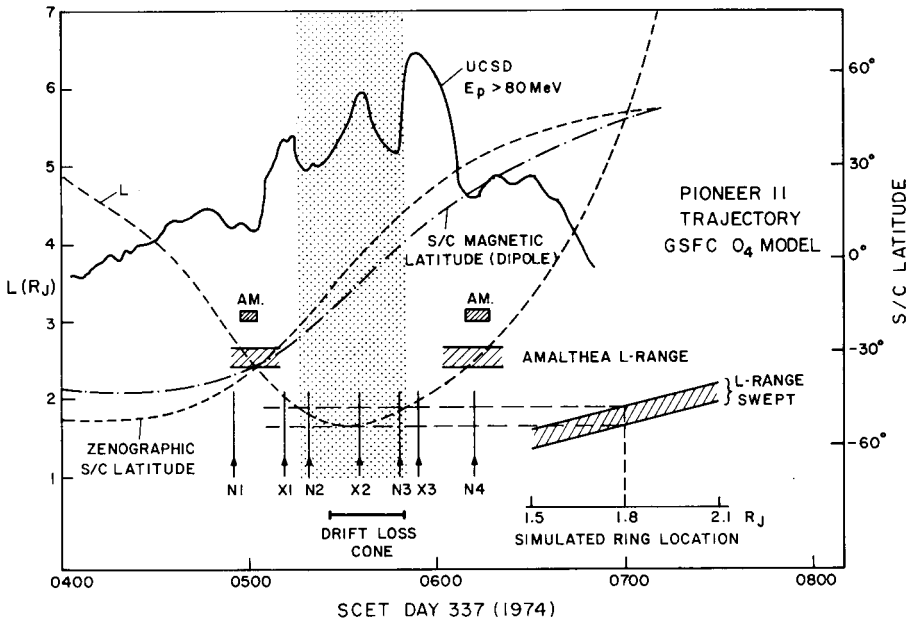

Fig. 1.9. Pioneer 11 observations of the Jovian ring. The charged particle data is that of Fillius [1976]. The L-values along the trajectory of Pioneer 11 and Amalthea were calculated using the O_4 model. A narrow ring located at 1.8 R_J provides an excellent fit to the observed absorption features N2 and N3.

One of the most interesting applications of adiabatic particle motion principles and satellite sweeping effects was the anticipation of the existence of a ring of particles around Jupiter at 1.8 R_J [Acuña and Ness, 1976c; Fillius, 1976; McLaughlin, 1980]. This is illustrated in Figure 1.9 where the Pioneer 11 spacecraft trajectory near closest approach in L-space and magnetic latitude is shown. Also shown are the energetic particle data of Fillius, Mogro-Campero, and McIlwain [1975] illustrating the existence of a multiply peaked structure in the count rate near closest approach. The two outer minima in the curve are due to absorption of energetic particles by Amalthea and correspond very closely to Amalthea's L-shell. The two inner minima are adequately explained by assuming the existence of a narrow absorber at 1.8 R_J, as indicated in the figure. This narrow ring was later observed by the Voyager 1 imaging experiment [Smith et al., 1979b]. The interpretation of the two minima being due to the presence of an absorber (ring or satellite) was considered remote since planetary rings had only been observed at Saturn [McLaughlin, 1980]. An analysis of the idealized response of energetic charged particle detectors aboard P 11 in an ambient magnetic field given by the O_4 model by Roederer, Acuña, and Ness [1977] indicated that the absorption signature could also be associated with geometric effects due to the intersection of the drift loss cone [Roederer, 1970] with the angular response of the detectors. This effect is indeed operative close to the planet but absorption by the ring material is the dominant loss mechanism.

It is also instructive to compute the configuration of the intersections of particle drift shells with the planetary ionosphere in order to locate areas where the mirror points for the trapped particles are low enough in altitude to interact strongly with the atmosphere–ionosphere. Constant L contours computed for the O_4 model are shown in